Article

Antigout and Antidiabetes Potentials of *Celastrus hindsii*

[Tran Duc Viet](#) *

Article

Antigout and Antidiabetes Potentials of *Celastrus hindsii*

Tran Duc Viet

Research and Development Department of Owarai Company Limited Company, Saijou Higashi, Hiroshima, 739-0014, Japan; tranducviet6868@gmail.com

Abstract

Background/Objectives: Given the growing global health threat posed by gout and diabetes, studying medicinal plants like *Celastrus hindsii* for their potential in supporting and treating these diseases is highly valuable. **Methods**: In this study, *Celastrus hindsii* leaves were extracted using different solvents, and their antihyperuricemic, α-amylase, and α-glucosidase inhibitory activities were evaluated. To gain deeper insights into the medicinal potential of this plant, gas chromatography - mass spectrometry(GC-MS) and Electrospray Ionization Mass Spectrometry (ESI-MS) analyses were performed to identify the bioactive compounds present in the extracts. **Results**: The results indicated that the ethyl acetate (EtOAc) extract demonstrated the most potent inhibitory effects against XO (IC_{50} = 114.06 µg/mL), α-amylase (IC_{50} = 363.46 µg/mL), and α-glucosidase (IC_{50} = 689.09 µg/mL). Furthermore, the EtOAc extract was fractionated using column chromatography for detailed analysis. Among the fractions obtained, fraction V5, eluted with $CHCl_3$:MeOH (99:1), exhibited the strongest inhibitory activity against XO (IC_{50} = 38.22 µg/mL), α-amylase (IC_{50} = 68.00 µg/mL), and α-glucosidase (IC_{50} = 293.22 µg/mL). Gas chromatography–mass spectrometry (GC–MS) and electrospray ionization mass spectrometry (ESI–MS) analyses revealed a substantial amount of fucosterol in the leaves of *C. hindsii* (2.03 mg/g extract), with the highest concentration detected in fraction V5 (1.08 mg/g fraction). **Conclusions**: This research has opened up the promising avenue for the development of *C. hindsii* as a valuable source for medicinal and functional food products.

Keywords: *Celastrus hindsii*; Xathine Oxidase; α- Amylase and α- Glucosidase; Fucosterol; GC-MS; ESI-MS

1. Introduction

Celastrus hindsii Benth, a species belonging to the *Celastraceae* family, is distributed in South America, China, and several Southeast Asian countries [1]. In Vietnam, *C. hindsii* grows naturally in forests and is cultivated in provinces such as Hoa Binh, Ha Nam, Quang Ninh, and Ninh Binh. Traditionally, this plant has been used in folk medicine for the treatment of cancer, ulcers, tumors, and inflammation [2]. Phytochemical studies have identified several bioactive compounds in the leaves of *C. hindsii*, including maytenfolone-A and celasdin-B, which exhibit anticancer and anti-HIV activities. The structure of maytenfolone-A was confirmed by X-ray crystallography. Biological evaluations revealed that maytenfolone-A shows cytotoxic activity against hepatoma (HEPA-2B, ED_{50} = 2.3 µg/mL) and nasopharyngeal carcinoma (KB, ED_{50} = 3.8 µg/mL) cell lines. Moreover, celasdin-B was found to inhibit HIV replication in H9 lymphocyte cells with an EC_{50} of 0.8 µg/mL [3]. Several antitumor agents from the *Celastraceae* family have also been reported, including cytotoxic sesquiterpene pyridine alkaloids. For instance, celahinine A, isolated from the ethanolic stem extract, showed potent cytotoxicity in vitro against various human cancer cell lines, including Hepa-2 (hepatoma), HeLa (cervical carcinoma), Colo 205 (colon carcinoma), and KB (nasopharyngeal carcinoma) [4]. The leaves of *C. hindsii* are also rich in total phenolic and flavonoid contents, contributing to their strong antioxidant potential [5]. Antioxidative compounds isolated from the 50% methanolic extract of dried *C. hindsii* leaves exhibited significant activity against the autoxidation of

methyl linoleate in bulk phase, as well as the radical-induced peroxidation of soybean phosphatidylcholine in liposome systems [2]. Furthermore, three new diphenylpropanes, Hindsiipropane A–C (1–3), along with a known arylpropyl quinone, Griffithane D (4), were isolated from *C. hindsii*. These compounds were evaluated in vitro for cytotoxicity against four human tumor cell lines (A549, HCT116, MDA-MB-231, and BEL7404) using the MTT assay [6].

Gout is a prevalent inflammatory arthritis characterized by hyperuricemia and the deposition of monosodium urate crystals in joints [7]. Gout is a common condition that is increasing worldwide, especially among men and younger people. The World Health Organization (WHO) estimates that it affects about 1 - 4% of the global population [8]. In the GBD 2021 report, as of 2020, approximately 55.8 million people worldwide had gout, with an age-standardized prevalence of 659.3 cases per 100,000 population, representing an increase of 22.5% compared to 1990. The projection shows that by 2050, the total number of gout cases globally could reach 95.8 million, representing an increase of more than 70% compared to 2020 [9]. In adults aged ≥ 55 years, the prevalence of gout has increased markedly. In 2021, this age group accounted for approximately 5.5 million cases, corresponding to an age-standardized prevalence rate of 2,505.4 per 100,000 population and an estimated average annual percent change (EAPC) of 1.08 % [10]. Gout exhibits a marked gender disparity, with men being 3.26 times more likely to be affected than women, and its risk increases progressively with age [11]. The major risk factors for gout include a purine-rich diet (such as meat and seafood), excessive alcohol intake, obesity, diabetes, kidney disease, and psoriasis. In recent years, the disease has also become increasingly prevalent among younger individuals, primarily attributable to sedentary lifestyles and unhealthy dietary patterns [12]. If left untreated, gout may result in serious complications, including chronic arthritis, joint damage, kidney stones, and kidney failure. Major factors contributing to the global increase in gout include high-protein diets, alcohol consumption, and sedentary lifestyles [12]. Gout is now recognized as a fast-rising public health problem globally. Forecasts predict that the patient population could more than double within the next decade, underscoring the urgent necessity for preventive strategies, lifestyle interventions, and enhanced treatment availability to mitigate its growing burden [13].

Diabetes mellitus is a chronic and serious metabolic disorder with multiple causes, marked by abnormalities in the metabolism of carbohydrates, fats, and proteins, resulting from either inadequate insulin production or impaired insulin action [14]. Diabetes mellitus is characterized by persistent hyperglycemia caused by defects in insulin secretion, insulin action, or both [15]. Over time, this elevated blood glucose results in damage, dysfunction, and eventual failure of multiple organs, particularly the eyes, kidneys, nerves, heart, and blood vessels [16]. According to the International Diabetes Federation (IDF), in 2021 an estimated 537 million adults aged 20–79 worldwide were living with diabetes, accounting for about 10.5% of the population in this age group [17]. The number of people with diabetes is projected to rise to 643 million by 2030 and 783 million by 2045, equivalent to roughly 1 in 8 adults worldwide [18]. Undiagnosed prevalence: Worldwide, approximately 44.7% of people with diabetes are undiagnosed, with the burden being particularly high in low- and middle-income countries [19]. According to the IDF Diabetes Atlas 2024, diabetes caused approximately 3.4 million deaths in 2024 equivalent to one death every nine seconds and generated global health expenditures of at least USD 1 trillion [20]. Diabetes is also one of the leading causes of coronary heart disease, stroke, blindness, renal failure, and impotence [21]. The worldwide increase in diabetes prevalence has severely impacted both human health and socio-economic development in numerous countries [22].

This study aimed to evaluate the potential of Celastrus hindsii as a herbal candidate for the treatment of gout and diabetes mellitus. To this end, enzyme inhibition assays were performed targeting xanthine oxidase (XO), α-amylase, and α-glucosidase, which play key roles in the pathophysiology of these metabolic disorders. In addition, the bioactive compound(s) responsible for the most potent inhibitory activity were identified and quantified using gas chromatography–mass spectrometry (GC-MS) and electrospray ionization mass spectrometry (ESI-MS).

2. Results

As shown in Table 1, the EtOAc extract exhibited the strongest inhibitory activities against XO, α-glucosidase, and α-amylase. Notably, XO inhibition by the EtOAc extract was characterized by an IC_{50} value of 114.06 µg/mL.

Table 1. XO, α - glucosidase, α-amylase inhibitory activities of *C. hindsii* extracts.

Extract	IC_{50} XO Inhibition (µg /mL)	IC_{50} α-Glucosidase Inhibition (µg /mL)	IC_{50} α-Amylase Inhibition (µg /mL)
EtAOC	114.06 ± 7.04[c]	363.46 ± 1.55[a]	689.09 ± 2.09 [a]
Aqueous	410.81 ± 6.89[b]	-	-
Haxane	621.11 ± 16.36[a]	-	-
Allopurinol	6.06 ± 0.38[d]	-	-
Acarbose	-	141.06 ± 0.64[b]	74.18 ± 4.21[b]

Data presented means ± standard deviation (SD). Mean within same column followed by similar letters are not significantly different by Turkey's test (p < 0.05). n.d. - = not determined.

The results in Table 2 indicate that fraction V5 (CHCl₃:MeOH, 99:1) was the most active, exhibiting the strongest inhibitory effects against XO, α-glucosidase, and α-amylase, followed by fractions V2 and V4. XO inhibition was most pronounced in fraction V5, which showed the lowest IC_{50} value among all fractions. Fraction V5 also demonstrated the highest potency against α-glucosidase, again followed by V2 and V4. α-Amylase inhibition was observed in all three fractions, with fraction V5 exhibiting the greatest activity. Overall, fraction V5 displayed the strongest inhibitory effects against XO and α-glucosidase, with the lowest IC_{50} values across the tested fractions.

Table 2. XO, α – glucosidase, α-amylase inhibitory activities of *C. hindsii* fractions.

Fractions	IC_{50} XO Inhibition (µg/mL)	IC_{50} α-Glucosidase Inhibition (µg/mL)	IC_{50} α-Amylase Inhibition (µg/mL)
V2	-	128.00 ± 7.12[c]	597.38 ± 3.94[a]
V4	-	185.00 ± 2.30[a]	
V5	38.22 ± 3.17[a]	68.00 ± 3.30[d]	292.33 ± 7.80[b]
Allopurinol	7.58 ± 1.29[b]	-	
Acarbose	-	145.06 ± 6.43[b]	74.18 ± 4.2[c]

Data discribed mean ± standard deviation (SD). Mean within same colunm followed by similar letter are not significantly different by Turkey's test (p<0.05). n.d - = not determined.

GC-MS results presented in Table 3 indicate that major compounds were distributed across the fractions, confirming their bioactivity. Notably, fucosterol was detected in all fractions with a high relative abundance.

Table 3. Principal compounds identified in fraction by GC-MS and ESI-MS.

Fraction	Time (min)	Area (% of total)	Compounds	Formula	Molecular Weight (g/mol)	Chemical Class
V2	21.27	32.17	Fucosterol	$C_{29}H_{48}O$	412.70	Phytosterols
	29.04	25.66	β-Amyrin	$C_{30}H_{50}O$	426.70	Triterpene
	29.67	36.09	α-Amyrin	$C_{30}H_{50}O$	426.70	Triterpene
V4	2.64	1.25	Fucosterol	$C_{29}H_{48}O$	412.70	Phytosterols
	21.28	38.64	Hydrazinecarboxamide	CH_5N_3O	75.07	Amino
	29.03	25.56	β-Amyrin	$C_{30}H_{50}O$	426.70	Triterpene
	29.64	32.71	α-Amyrin	$C_{30}H_{50}O$	426.70	Triterpene
V5	21.28	34.22	Bauerenol	$C_{30}H_{50}O$	426.70	Triterpenoid
	21.45	43.62	Fucosterol	$C_{29}H_{48}O$	412.70	Sterol

| 22.10 | 4.78 | β-Amyrin | $C_{30}H_{50}O$ | 426.70 | Triterpene |
| 29.68 | 8.55 | α-Amyrin | $C_{30}H_{50}O$ | 426.70 | Triterpene |

The results in Table 4 indicate that fucosterol is a potent inhibitor of XO, α-glucosidase, and α-amylase. Its XO inhibitory activity was characterized by an IC$_{50}$ of 5.28 µg/mL, surpassing that of the allopurinol standard (IC$_{50}$ = 7.58 µg/mL). Additionally, fucosterol exhibited significant anti-diabetic potential, with IC$_{50}$ values of 58.22 µg/mL for α-glucosidase inhibition (compared to acarbose, IC$_{50}$ = 155.25 µg/mL) and 88.55 µg/mL for α-amylase inhibition.

Table 4. XO, α - glucosidase, α-amylase inhibitory activities of fucosterol.

Fractions	IC$_{50}$ XO Inhibition (µg /mL)	IC$_{50}$ α-Glucosidase Inhibition (µg /mL)	IC$_{50}$ α-Amylase Inhibition (µg /mL)
Fucosterol	5.28 ± 1.22[b]	58.22 ± 2.18[b]	88.55 ± 2.88[a]
Allopurinol	7.58 ± 1.05[a]	-	-
Acarbose	-	155.28 ± 5.88[a]	72.25 ± 2.25[c]

Data presented means ± standard deviation (SD). Means within same column followed by similar letters are not significantly different by Turkey's test (p < 0.05). n.d. - = not determined.
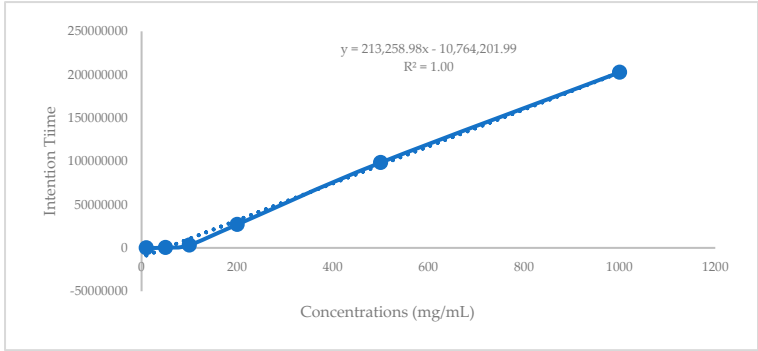

Figure 1. Fucosterol quantitation standard curve graph.

The quantification of fucosterol in *C. hindsii* leaves was performed using a standard curve equation (y = 213,258.98x − 10,764,201.99) (Figure 1). Six different concentrations of fucosterol standard were analyzed using the GC-MS system, and the retention time data were used to construct the standard curve. The retention times of fucosterol in the fractions were applied to the standard curve for quantification. Fraction V5 exhibited the highest fucosterol content at 1.08 mg/g fraction, followed by V4 (0.84 mg/g) and V2 (0.51 mg/g) (Table 5). Based on these results, the total fucosterol content in the leaves of C. hindsii was substantial, reaching 2.03 mg/kg extract.

Table 5. The results of quantification fucosterol in *fractions*.

Fractions	Intention Time (Second/ g)	Concentration (mg/g)
V2	98412933.03	0.51
V4	168641969.5	0.84
V5	221163634	1.08
Total in leaves of *C.hindsii*		(2.03 mg/ kg extract)

3. Discussion

C. hindsii is a valuable medicinal plant with potential preventive properties against inflammatory diseases and tumors [23]. It has been reported to exhibit diverse biological activities [24]. The leaves of *C. hindsii* possess strong antioxidant potential, being rich in numerous compounds

with therapeutic and curative value [25]. The present study further emphasizes its promising anti-gout and anti-diabetic potentials, thereby supporting its traditional use as a medicinal plant. The observed anti-gout effect may be attributed to the inhibitory activity of bioactive constituents on xanthine oxidase, the key enzyme responsible for uric acid production [26]. In addition, the inhibition of α-amylase and α-glucosidase by *C. hindsii* suggests its ability to regulate postprandial blood glucose levels, a crucial therapeutic target in type 2 diabetes management. Such mechanisms are comparable to those of standard antidiabetic agents, such as acarbose, further highlighting its potential as a natural source of enzyme inhibitors [27]

Xanthine oxidase (XO) is a key enzyme in purine metabolism that catalyzes the sequential oxidation of hypoxanthine to xanthine and subsequently to uric acid [28]. Inhibition of XO reduces uric acid production, thereby lowering serum uric acid levels and contributing to the prevention and management of gout [29]. The results presented in Tables 1 and 2 demonstrate the ability of *C. hindsii* to inhibit XO activity, supporting its potential as a natural anti-gout agent.

α-Amylase is an enzyme found in both saliva and pancreatic juice, where it plays a crucial role in the breakdown of dietary starch into smaller sugars [30]. It catalyzes the hydrolysis of starch into oligosaccharides, which are subsequently converted into maltose and ultimately into glucose [31]. The resulting glucose is absorbed into the bloodstream, leading to postprandial hyperglycemia [32]. Natural compounds such as flavonoids, triterpenoids, and alkaloids are known to inhibit α-amylase activity [33]. Inhibition of this enzyme slows the breakdown of starch, thereby delaying glucose production and absorption. Consequently, postprandial blood glucose levels rise more gradually rather than spiking abruptly, which contributes to improved glycemic control and supports the management of type 2 diabetes [34]. The results in Tables 1 and 2 demonstrate the inhibitory potential of *C. hindsii* extract and its fractions against α-amylase activity. Based on this mechanism, *C. hindsii* can be regarded as a promising medicinal plant for supporting diabetes management.

α-Glucosidase is an intestinal enzyme that catalyzes the hydrolysis of disaccharides into glucose [35]. In the digestive tract, complex carbohydrates (starches) must be hydrolyzed into simple sugars for absorption, a process in which α-glucosidase plays a crucial role [36]. Inhibition of this enzyme slows carbohydrate breakdown, thereby delaying glucose absorption in the small intestine and lowering postprandial blood glucose levels [37]. α-Glucosidase inhibitors, such as acarbose, voglibose, and miglitol, are widely used antidiabetic agents that act through this mechanism [38–40]. However, these drugs are often associated with gastrointestinal side effects, including bloating, diarrhea, and flatulence [41], and in certain cases—particularly in elderly patients or those with a history of gastrointestinal surgery—they may even lead to intestinal obstruction. Thus, their clinical use requires caution [42]. The results presented in Tables 1 and 2 demonstrate the α-glucosidase inhibitory activity of *C. hindsii*, highlighting its potential as a natural antidiabetic agent and a promising candidate for the development of supportive therapies in diabetes management.

Fucosterol is a naturally occurring phytosterol predominantly found in brown seaweeds, and to a lesser extent in other plant sources [43]. It exhibits diverse biological activities, including antioxidant, anti-inflammatory, anticancer, and antidiabetic effects, highlighting its potential therapeutic applications [44]. Fucosterol has been reported to reduce markers of oxidative damage and support glycemic regulation, including lowering serum glucose levels in diabetic animal models [45]. As shown in Table 3, the presence of fucosterol was confirmed in the fractions, while Table 4 demonstrates its potent anti-gout and antidiabetic activities. Notably, in vitro experiments revealed stronger effects than those of current standard therapeutic agents, providing important evidence for the role of fucosterol in the antidiabetic properties of *C. hindsii* and its fractions. Although the concentration of fucosterol in *C. hindsii* is relatively low, its contribution to the plant's biological activities is significant. Importantly, fucosterol has been demonstrated to be non-toxic [46]. No toxic effects have been observed in animal models at doses ranging from 10 to 100 mg/kg/day [47], and it is non-toxic to various cell lines, including hepatocytes (HepG2) at concentrations up to 100 μM, where it even provides protection against oxidative stress [48]. These findings further underscore the potential of *C. hindsii* in supporting the management of diabetes and gout.

α-Amyrin and β-amyrin are triterpene compounds widely distributed in plants, including the roots of *Abutilon indicum*, the leaves of *Celastrus hindsii*, and the roots of *Lactuca indica L.* They are reported to possess significant anti-inflammatory and cholesterol-lowering activities [49]. Amyrin extracted from *C. hindsii* has demonstrated anti-gout potential through xanthine oxidase (XO) inhibition, with an IC_{50} value of 258.22 μg/mL [50]. Both α- and β-amyrin reduced serum uric acid levels in a hyperuricemic animal model by inhibiting hepatic XO, thereby supporting their potential in gout prevention and treatment [51]. In a streptozotocin (STZ)-induced diabetic mouse model, administration of a mixture of α- and β-amyrin (10, 30, and 100 mg/kg) significantly reduced blood glucose, total cholesterol, and triglyceride levels, showing effects comparable to glibenclamide and fenofibrate. At 100 mg/kg, the mixture also improved LDL and VLDL cholesterol levels, increased HDL cholesterol, and protected pancreatic β-cells [52]. In an oral glucose tolerance test, α- and β-amyrin lowered blood glucose levels, indicating enhanced glucose metabolism [53]. In C2C12 myoblasts, α-amyrin activated both PPARδ and PPARγ receptors, enhanced AMPK phosphorylation, and promoted GLUT4 translocation, thereby increasing glucose uptake. These findings suggest that α-amyrin exerts insulin-like effects and may contribute to glycemic control in type 2 diabetes [54]. In a high-fructose diet mouse model, α-amyrin (50–200 mg/kg) prevented hyperglycemia, improved glucose and insulin tolerance, reduced hepatic oxidative stress, and preserved PPAR-α expression, thus mitigating metabolic disturbances induced by an unhealthy diet [55]. In a diabetic kidney injury mouse model, β-amyrin reduced inflammation and apoptosis in renal tubular cells by modulating the miR-181b-5p/HMGB2 axis, thereby protecting against diabetic nephropathy [56]. Combination therapy of β-amyrin with metformin in hyperglycemic zebrafish markedly reduced blood glucose (~104 mg/dL vs. ~389 mg/dL in controls), improved renal function, and decreased intracellular stress, endoplasmic reticulum stress, apoptosis, and inflammation, showing superior efficacy compared with either treatment alone [57]. α-Amyrin acetate, isolated from *Ficus racemosa* fruit, reduced blood glucose by ~17–18% in an STZ-sucrose-induced diabetic rat model at 100 mg/kg, while derivatives such as p-chlorobenzoic and nicotinic acid exhibited even greater glucose-lowering activity [58]. β-Amyrin palmitate, isolated from *Hemidesmus indicus* roots, also demonstrated significant antihyperglycemic activity in alloxan- and STZ-induced diabetic rat models, as well as in glucose tolerance tests [59]. The detection of α- and β-amyrin in the fractions of *C. hindsii* (Table 3) provides strong evidence for its anti-gout and antidiabetic potential. The amyrin content in *C. hindsii* was determined to be 10.75 g/kg dry weight [50]. Furthermore, amyrin has been shown to be non-toxic to cells [51], further supporting the potential of *C. hindsii* in the management of diabetes and gout. This study demonstrated the anti-gout and anti-diabetic activities of *C. hindsii*. Although the findings are limited to the in vitro level, they highlight the significant potential of *C. hindsii* and provide a foundation for further investigations in vivo and at the clinical level

4. Materials and Methods

4.1. Materials

The plant materials of C. hindsii were collected in Cao Duong Commune, Luong Son District, Hoa Binh Province, Vietnam. Fifty mature plants, each over five years old, were randomly selected for leaf harvesting. These plants had grown naturally, were healthy, pest- and disease-free, and had never been treated with fertilizers, pesticides, or growth stimulants. The collected materials were authenticated and sterilized, with specimens (No. PPBC170506) preserved for subsequent experiments.

4.2. Preparation of Plant Extract

An amount of 1.12 kg of *C. hindsii* leaves was re-dried in a tray at 40 °C for two days and subsequently ground into a fine powder using a mill. The resulting powder was macerated in 10 L of methanol (MeOH) at room temperature for three weeks. The extract solution was then filtered and concentrated under reduced pressure at 45 °C using a rotary evaporator (SB-350-EYELA, Tokyo

Rikakikai Co., Ltd., Tokyo, Japan), yielding 230 g of crude extract. To isolate plant growth inhibitors with different polarities, the crude methanol extract was suspended in 500 ml of water and successively partitioned with ethyl acetate (EtOAc) and hexane, producing 55.30 g aqueous, 133.33 g EtOAc, and 33.32 g hexane extracts, respectively. These extracts were subsequently subjected to further separation using column chromatography.

4.3. Fractionation of Ethyl Acetate Fraction

The EtOAc fraction (133.33 g), which exhibited the strongest inhibitory activity in preliminary assays, was subjected to normal-phase column chromatography (20 mm diameter × 500 mm height, Climbing G2, Tokyo, Japan) using silica gel (size A 60, 200–400 mesh, Sigma Aldrich) as the stationary phase. Elution was performed sequentially with solvent systems of increasing polarity, yielding 14 fractions: V1 ($CHCl_3$), V2–V6 [$CHCl_3$:MeOH (9.9:0.1), flasks 1–20, 21–40, 41–60, 61–80, and 81–100, respectively], V7 ($CHCl_3$:MeOH, 97:3), V8 ($CHCl_3$:MeOH, 95:5), V9 ($CHCl_3$:MeOH, 9:1), V10 ($CHCl_3$:MeOH, 8:2), V11 ($CHCl_3$:MeOH, 7:3), V12 ($CHCl_3$:MeOH, 5:5), V13 ($CHCl_3$:MeOH, 3:7), and V14 ($CHCl_3$:MeOH, 1:9).

4.4. Xanthine Oxidase (XO) Inhibitory Activity

The xanthine oxidase (XO) inhibitory activity was determined in vitro under aerobic conditions using a spectrophotometric assay at 290 nm [60]. Briefly, 50 μL of the test solution was mixed with 35 μL of 70 mM phosphate buffer (pH 7.5) and 30 μL of freshly prepared enzyme solution (0.01 U/mL in 70 mM phosphate buffer, pH 7.5). After pre-incubation at 25 °C for 15 min, the reaction was initiated by adding 60 μL of substrate solution (150 μM xanthine in the same buffer). The assay mixture was incubated at 25 °C for 30 min, and the reaction was terminated by adding 25 μL of 1 M HCl. Absorbance was then measured at 290 nm using a microplate reader (Multiskan Microplate Spectrophotometer, Thermo Fisher Scientific, Osaka, Japan).

For the blank, the assay mixture was prepared under the same conditions, except that the enzyme solution was added only after HCl addition. One unit of XO activity was defined as the amount of enzyme required to produce 1 μmol of uric acid per minute at 25 °C. XO inhibitory activity was expressed as the percentage inhibition of XO in the above assay system and calculated using the following formula:

$$\% \text{ Inhibition} = \left\{ \frac{(A-B)-(C-D)}{A-B} \right\} \times 100 \tag{1}$$

where A is the activity of the enzyme without test extract or fraction, B is the control of A without test extract or fraction and enzyme, C and D are the activities of the test extract or fraction with and without XO. Allopurinol (10-100 μg/mL) was used as a positive control. IC_{50} values were calculated from the mean values of percentage inhibition data.

4.5. Porcine Pancreatic α-Glucosidase Inhibition Assay

The α-glucosidase inhibitory activity of TDB extracts was evaluated using a modified version [61]. Briefly, 40 μL of TDB extract prepared in 0.1 M potassium phosphate buffer (pH 7.0) was pre-incubated with 40 μL of α-glucosidase solution (0.5 U/mL, from *Saccharomyces cerevisiae*, Sigma-Aldrich, St. Louis, MO, USA) at 25 °C for 6 min. The reaction was initiated by adding 20 μL of 5 mM *p*-nitrophenyl-D-glucopyranoside (pNPG) substrate in the same buffer, followed by incubation for an additional 8 min. The reaction was terminated with 100 μL of 0.1 M Na_2CO_3, and absorbance was measured at 405 nm.

The inhibitory activity was expressed as a percentage of α-glucosidase inhibition and calculated using the following equation:

$$\% \text{ Inhibition} = (1 - A_{sample}/A_{control}) \times 100$$

where Asample is absorbance of the reaction with samples or positive controls (acarbose) and Acontrol is absorbance of reaction with 10% methanol. The enzymatic inhibitory activity of TDB extracts was expressed as IC_{50} value as well.

4.6. Porcine Pancreatic a-Amylase Inhibition Assay

The α-amylase inhibitory activity was evaluated using the starch–iodine method. α-Amylase solution (2 mg/mL, from porcine pancreas, type VI-B, Sigma-Aldrich, St. Louis, MO, USA) and TDB extracts were prepared in 0.2 M phosphate buffer saline (pH 6.9). Solutions of iodine (0.25 mM) and soluble starch (0.5%) were prepared in deionized water. Briefly, 20 µL of α-amylase solution was mixed with 20 µL of the test sample and incubated at 37 °C for 10 min. Subsequently, 30 µL of soluble starch solution was added, followed by an additional incubation for 8 min. The reaction was terminated by adding 20 µL of 1 M HCl, after which 100 µL of iodine solution was added. Absorbance was measured at 565 nm using a microplate reader. The percentage inhibition and IC_{50} value were determined as described previously, with acarbose serving as the positive control [62].

4.7. Pharmaceutical compounds identification by Gas Chromatography–Mass Spectrometry (GC–MS)

The chemical constituents of the fractions were analyzed using a GC–MS system (JMS-T100 GCV, JEOL Ltd., Tokyo, Japan). A 1 µL aliquot of each sample, dissolved in methanol, was injected into the system. Separation was performed on a DB-5MS capillary column (30 m × 0.25 mm i.d., 0.25 µm film thickness; Agilent Technologies, J & W Scientific Products, Folsom, CA, USA). Helium was used as the carrier gas with a split ratio of 5:1. The GC oven program was as follows: initial temperature of 50 °C (no hold), ramped at 10 °C/min to 300 °C, and held for 20 min. Injector and detector temperatures were set at 300 °C and 320 °C, respectively. Mass spectra were recorded over a scan range of 29–800 amu. System control and data processing were performed using JEOL GC–MS Mass Center System software (version 2.65a). Compounds representing peak areas greater than 0.3% in the GC–MS chromatogram were considered principal constituents **[63]**

4.8. Electrospray Ionization-Mass Spectrometry (ESI-MS) Analysis.

ESI-MS analysis was conducted on negative/positive ino mode. The capillary temperature was set up of 140 ºC (120 ºC for S2) and spray voltage of 3.0KV (2.7Kv for S2). The measurements were performed in the positive mode with an ion spray voltage of 3000V and capillary temperature of 350 ºC. Data peak were scanned within the range 280 to 1000m/z [64]

4.9. Statistical Analysis

Statistical analyses were conducted using one-way ANOVA with Minitab® version 16.2.3 (©2012, Minitab Inc., Philadelphia, PA, USA). Tukey's test was employed to identify significant differences ($p < 0.05$) among the tested samples. Results are presented as mean values ± standard error (SE).

5. Conclusions

This study was important document to express potential of XO, α-amylase and α- glucosidase inhibitory activities of *C. hindsii.* Fractions of ethyl acetate with huge of fucosterol amount was new findings. Fraction V5 (CM; 99: 1) F_{37-44} showed potent pharmaceutical properties, was the most XO, α-amylase and α-glucosidase inhibitory. These are extremely valuable signals to consolidate the development of *C. hindsii* into a practical medicinal source for the treatment of gout and diabetes.

6. Patents

Author Contributions: Tran Duc Viet conducted the experiments and wrote the manuscript , supervised and corrected the revised version.

Conflicts of Interest: The authors declare no conflict of interest.

References

1. Spivey, A.C.; Weston, M.; Woodhead, S. Celastraceae sesquiterpenoids: Biological activity and synthesis. *Chem. Soc. Rev.* **2002**, *31*, 43–59.
2. Ly, T.N.; Shimoyamada, M.; Yamauchi, R. Isolation and characterization of rosmarinic acid oligomers in *Celastrus hindsii* Benth leaves and their antioxidative activity. *J. Agric. Food Chem.* **2006**, *54*, 3786–3793.
3. Kuo, Y.H.; Kuo, L.M.Y. Antitumour and anti-AIDS triterpenes from *Celastrus hindsii. Phytochemistry.* **1997**, *44*, 1275–1281.
4. Viet, T.D.; Xuan, T.D.; Van, T.M.; Andriana, Y.; Rayee, R.; Tran, H.D. Comprehensive fractionation of antioxidants and GC-MS and ESI-MS fingerprints of *Celastrus hindsii* leaves. *Medicines.* **2019**, *6*, 64.
5. Hu, X.Q.; Han, W.; Han, Z.Z.; Liu, Q.X.; Xu, X.K.; Fu, P.; Li, H.L. Three new diphenylpropanes from *Celastrus hindsii. Arch. Pharm. Res.* **2014**, *37*, 1411–1415.
6. Hu, X.Q.; Han, W.; Han, Z.Z.; Liu, Q.X.; Xu, X.K.; Fu, P.; Li, H.L. Three new diphenylpropanes from *Celastrus hindsii. Arch. Pharm. Res.* **2014**, *37*(11), 1411–1415.
7. Parthasarathy, P.; Vivekanandan, S. Urate crystal deposition, prevention and various diagnosis techniques of gout arthritis disease: A comprehensive review. *Health Inf. Sci. Syst.* **2018**, *6*, 19.
8. Han, T.; Chen, W.; Qiu, X.; Wang, W. Epidemiology of gout–Global burden of disease research from 1990 to 2019 and future trend predictions. *Ther. Adv. Endocrinol. Metab.* **2024**, *15*, 20420188241227295.
9. Cross, M.; Ong, K.L.; Culbreth, G.T.; Steinmetz, J.D.; Cousin, E.; Lenox, H.; Woolf, A.D. Global, regional, and national burden of gout, 1990–2020, and projections to 2050: A systematic analysis of the Global Burden of Disease Study 2021. *Lancet Rheumatol.* **2024**, *6*, e507–e517.
10. Li, Y.; Chen, Z.; Xu, B.; Wu, G.; Yuan, Q.; Xue, X.; Mo, S. Global, regional, and national burden of gout in elderly 1990–2021: An analysis for the global burden of disease study 2021. *BMC Public Health.* **2024**, *24*, 3298.
11. Li, M.; Nie, Q.; Xia, Q.; Jiang, Z. Assessing cross-national inequalities and predictive trends in gout burden: A global perspective (1990–2021). *Front. Med.* **2025**, *12*, 1527716.
12. Singh, J.A.; Reddy, S.G.; Kundukulam, J. Risk factors for gout and prevention: A systematic review of the literature. *Curr. Opin. Rheumatol.* **2011**, *23*, 192–202.
13. Engel, B.; Just, J.; Bleckwenn, M.; Weckbecker, K. Treatment options for gout. *Dtsch. Arztebl. Int.* **2017**, *114*, 215.
14. Sarkar, B.K.; Akter, R.; Das, J.; Das, A.; Modak, P.; Halder, S.; Kundu, S.K. Diabetes mellitus: A comprehensive review. *J. Pharmacogn. Phytochem.* **2019**, *8*, 2362–2371.
15. Tripathy, D.; Chavez, A.O. Defects in insulin secretion and action in the pathogenesis of type 2 diabetes mellitus. *Curr. Diabetes Rep.* **2010**, *10*, 184–191.
16. Mezil, S.A.; Abed, B.A. Complication of diabetes mellitus. *Ann. Rom. Soc. Cell Biol.* **2021**, *25*, 1546–1556.
17. Kumar, A.; Gangwar, R.; Ahmad Zargar, A.; Kumar, R.; Sharma, A. Prevalence of diabetes in India: A review of IDF diabetes atlas 10th edition. *Curr. Diabetes Rev.* **2024**, *20*, 105–114.
18. Yameny, A.A. Diabetes mellitus overview 2024. *J. Biosci. Appl. Res.* **2024**, *10*, 641–645.
19. Ogurtsova, K.; Guariguata, L.; Barengo, N.C.; Ruiz, P.L.D.; Sacre, J.W.; Karuranga, S.; Magliano, D.J. IDF diabetes Atlas: Global estimates of undiagnosed diabetes in adults for 2021. *Diabetes Res. Clin. Pract.* **2022**, *183*, 109118.
20. Wagh, K.; Kirpich, A.; Chowell, G. The future diabetes mortality: Challenges in meeting the 2030 Sustainable Development Goal of reducing premature mortality from diabetes. *J. Clin. Med.* **2025**, *14*, 3364.
21. Razaq, R.A.; Mahdi, J.A.; Jawad, R.A. Information about diabetes mellitus. *J. Univ. Babylon Pure Appl. Sci.* **2020**, *28*, 243–252.

22. Mutyambizi, C.; Booysen, F.; Stokes, A.; Pavlova, M.; Groot, W. Lifestyle and socio-economic inequalities in diabetes prevalence in South Africa: A decomposition analysis. *PLoS ONE*. **2019**, *14*, e0211208.

23. Aggarwal, B.B.; Prasad, S.; Reuter, S.; Kannappan, R.; Yadav, V.R.; Park, B.; Sung, B. Identification of novel anti-inflammatory agents from Ayurvedic medicine for prevention of chronic diseases: "Reverse pharmacology" and "bedside to bench" approach. *Curr. Drug Targets* **2011**, *12*(11), 1595–1653.

24. Do, D.T.; Hai, N.D.; Nam, N.T.H.; Thanh, N.M.; Huyen, N.T.T.; Duong, L.T.T.; Hieu, N.H. Flavonoid content and antifungal activity of *Celastrus hindsii* leaf extract obtained by supercritical carbon dioxide using ethanol as co-solvent. *Biocatal. Agric. Biotechnol.* **2023**, *52*, 102824.

25. Pham, T.L. An *in silico* approach for identification of potential therapeutic targets for cancer treatment from *Celastrus hindsii* Benth. *Malays. Appl. Biol.* **2024**, *53*(1), 35–42.

26. Ashiq, K.; Hussain, K.; Islam, M.; Shehzadi, N.; Ali, E.; Ashiq, S. Medicinal plants of Pakistan and their xanthine oxidase inhibition activity to treat gout: A systematic review. *Turk. J. Bot.* **2021**, *45*(8), 723–738.

27. Kashtoh, H.; Baek, K.H. Recent updates on phytoconstituent α-glucosidase inhibitors: An approach towards the treatment of type two diabetes. *Plants.* **2022**, *11*(20), 2722.

28. Bortolotti, M.; Polito, L.; Battelli, M.G.; Bolognesi, A. Xanthine oxidoreductase: One enzyme for multiple physiological tasks. *Redox Biol.* **2021**, *41*, 101882.

29. Alghamdi, A.A.; Althumali, J.S.; Almalki, M.M.M.; Almasoudi, A.S.; Almuntashiri, A.H.; Mahzari, M.A.H. An overview on the role of xanthine oxidase inhibitors in gout management. *Arch. Pharm. Pract.* **2021**, *12*(3), 94–99.

30. Zhang, Y.; Chen, Y.; Chen, J. The starch hydrolysis and aroma retention caused by salivary α-amylase during oral processing of food. *Curr. Opin. Food Sci.* **2022**, *43*, 237–245.

31. Dhital, S.; Warren, F.J.; Butterworth, P.J.; Ellis, P.R.; Gidley, M.J. Mechanisms of starch digestion by α-amylase—Structural basis for kinetic properties. *Crit. Rev. Food Sci. Nutr.* **2017**, *57*(5), 875–892.

32. Hiyoshi, T.; Fujiwara, M.; Yao, Z. Postprandial hyperglycemia and postprandial hypertriglyceridemia in type 2 diabetes. *J. Biomed. Res.* **2019**, *33*(1), 1–7.

33. Kartini, S.; Juariah, S.; Mardhiyani, D.; Bakar, M.F.A.; Bakar, F.I.A.; Endrini, S. Phytochemical properties, antioxidant activity and α-amylase inhibitory of *Curcuma caesia*. *J. Adv. Res. Appl. Sci. Eng. Technol.* **2023**, *30*(1), 255–263.

34. Li, X.; Bai, Y.; Jin, Z.; Svensson, B. Food-derived non-phenolic α-amylase and α-glucosidase inhibitors for controlling starch digestion rate and guiding diabetes-friendly recipes. *LWT.* **2022**, *153*, 112455.

35. Bhatnagar, A.; Mishra, A. α-Glucosidase inhibitors for diabetes/blood sugar regulation. In Natural Products as Enzyme Inhibitors: An Industrial Perspective. *Springer Nature: Singapore.* **2022**, 269–283

36. Li, X.; Bai, Y.; Jin, Z.; Svensson, B. Food-derived non-phenolic α-amylase and α-glucosidase inhibitors for controlling starch digestion rate and guiding diabetes-friendly recipes. *LWT.* **2022**, *153*, 112455.

37. Gromova, L.V.; Fetissov, S.O.; Gruzdkov, A.A. Mechanisms of glucose absorption in the small intestine in health and metabolic diseases and their role in appetite regulation. *Nutrients.* **2021**, *13*(7), 2474.

38. Arjita, I.P.D.; Yasa, I.W.P.S.; Dewi, N.N.A.; Satriyasa, B.K.; Suastika, K.; Saraswati, M.R.; Saputra, I.P.B.A. Potential α-glucosidase inhibitor in Nyale worm (*Eunice* sp.) extract for anti-diabetic type 2 target. *Regul. Mech. Biosyst.* **2024**, *15*(4), 900–906.

39. Barrett, A.H.; Farhadi, N.F.; Smith, T.J. Slowing starch digestion and inhibiting digestive enzyme activity using plant flavanols/tannins A review of efficacy and mechanisms. *LWT.* **2018**, *87*, 394–399.

40. Dash, R.P.; Babu, R.J.; Srinivas, N.R. Reappraisal and perspectives of clinical drug–drug interaction potential of α-glucosidase inhibitors such as acarbose, voglibose and miglitol in the treatment of type 2 diabetes mellitus. *Xenobiotica.* **2018**, *48*(1), 89–108.

41. Boland, B.S.; Edelman, S.V.; Wolosin, J.D. Gastrointestinal complications of diabetes. *Endocrinol. Metab. Clin. N. Am.* **2013**, *42*(4), 809–832.

42. Kashtoh, H.; Baek, K.H. Recent updates on phytoconstituent α-glucosidase inhibitors: An approach towards the treatment of type two diabetes. *Plants* **2022**, *11*(20), 2722.

43. Meinita, M.D.N.; Harwanto, D.; Tirtawijaya, G.; Negara, B.F.S.P.; Sohn, J.H.; Kim, J.S.; Choi, J.S. Fucosterol of marine macroalgae: Bioactivity, safety and toxicity on organism. *Mar. Drugs.* **2021**, *19*(10), 545.

44. Abdul, Q.A.; Choi, R.J.; Jung, H.A.; Choi, J.S. Health benefit of fucosterol from marine algae: A review. *J. Sci. Food Agric.* **2016**, *96*(6), 1856–1866.

45. Lee, Y.S.; Shin, K.H.; Kim, B.K.; Lee, S. Anti-diabetic activities of fucosterol from *Pelvetia siliquosa*. *Arch. Pharm. Res.* **2004**, *27*(11), 1120–1122.

46. Mourelle, M.L.; Gómez, C.P.; Legido, J.L. Role of algal derived compounds in pharmaceuticals and cosmetics. In Recent Advances in Micro and Macroalgal Processing: *Food and Health Perspectives.* **2021**, 537-603.

47. Hwang, J.; Kim, M.B.; Lee, S.; Hwang, J.K. Fucosterol, a phytosterol of marine algae, attenuates immobilization-induced skeletal muscle atrophy in C57BL/6J mice. *Mar. Drugs.* **2024**, *22*(12), 557.

48. Donato, M.T.; Jiménez, N.; Pelechá, M.; Tolosa, L. Oxidative-stress and long-term hepatotoxicity: Comparative study in Upcyte human hepatocytes and HepaRG cells. *Arch. Toxicol.* **2022**, *96*(4), 1021–1037.

49. Alsaedi, H.K.; Alwan, N.A.; Al-Masoudi, E.A. Physiological and biochemical effect of α-amyrin: A review. *J. Med. Life Sci.* **2024**, *6*(3), 443–452.

50. Viet, T.D.; Xuan, T.D.; Anh, L.H. α-Amyrin and β-amyrin isolated from *Celastrus hindsii* leaves and their antioxidant, anti-xanthine oxidase, and anti-tyrosinase potentials. *Molecules.* **2021**, *26*(23), 7248.

51. Viet, T.D.; Anh, L.H.; Xuan, T.D.; Dong, N.D. The pharmaceutical potential of α- and β-amyrins. *Nutraceuticals.* **2025**, *5*(3), 21.

52. Santos, F.A.; Frota, J.T.; Arruda, B.R.; de Melo, T.S.; da Silva, A.A.C.A.; Brito, G.A.C.; Rao, V.S. Antihyperglycemic and hypolipidemic effects of α,β-amyrin, a triterpenoid mixture from *Protium heptaphyllum* in mice. *Lipids Health Dis.* **2012**, *11*, 98.

53. Prabhakar, P.; Reeta, K.H.; Maulik, S.K.; Dinda, A.K.; Gupta, Y.K. α-Amyrin attenuates high fructose diet-induced metabolic syndrome in rats. *Appl. Physiol. Nutr. Metab.* **2017**, *42*(1), 23–32.

54. Sureka, D.; Sam Rosan, Y.; Avinash, B.; Blessy Victa, N.I.; Christi, V.I. A mechanism-based comparative review on functional food with phytomolecules and marketed formulation for type II diabetes mellitus. *Curr. Funct. Foods.* **2024**

55. da Silva Ferreira, R.G.; Guilhon-Simplicio, F.; Acho, L.D.R.; Batista, N.Y.; do Carmo Guedes-Junior, F.; Ferreira, M.S.L.; Lima, E.S. Anti-hyperglycemic, lipid-lowering, and anti-obesity effects of the triterpenes α- and β-amyrenones *in vivo*. *Avicenna J. Phytomed.* **2021**, *11*(5), 451-460.

56. Xu, W.; Zhang, H.; Zhang, Q.; Xu, J. β-Amyrin ameliorates diabetic nephropathy in mice and regulates the miR-181b-5p/HMGB2 axis in high glucose-stimulated HK-2 cells. *Environ. Toxicol.* **2022**, *37*(3), 637–649.

57. Roohi, T.F.; Krishna, K.L.; Shakeel, F. Synergistic modulation of endoplasmic reticulum stress pathway, oxidative DNA damage and apoptosis by β-amyrin and metformin in mitigating hyperglycemia-induced renal damage using adult zebrafish model. *BMC Pharmacol. Toxicol.* **2024**, *25*(1), 66.

58. Tomazi, R.; Figueira, Â.C.; Ferreira, A.M.; Ferreira, D.Q.; de Souza, G.C.; de Souza Pinheiro, W.B.; da Silva de Almeida, S.S.M. Hypoglycemic activity of aqueous extract of latex from *Hancornia speciosa* Gomes: A study in zebrafish and *in silico*. *Pharmaceuticals.* **2021**, *14*(9), 856.

59. Nair, S.A.; Sabulal, B.; Radhika, J.; Arunkumar, R.; Subramoniam, A. Promising anti-diabetes mellitus activity in rats of β-amyrin palmitate isolated from *Hemidesmus indicus* roots. *Eur. J. Pharmacol.* **2014**, *734*, 77–82.

60. Andriana, Y.; Xuan, T.D.; Quy, T.N.; Minh, T.N.; Van, T.M.; Viet, T.D. Antihyperuricemia, antioxidant, and antibacterial activities of *Tridax procumbens* L. *Foods.* **2019**, *8*(1), 21.

61. Anh, L.T.T.; Son, N.T.; Van Tuyen, N.; Thuy, P.T.; Quan, P.M.; Ha, N.T.T.; Tra, N.T. Antioxidative and α-glucosidase inhibitory constituents of *Polyscias guilfoylei*: Experimental and computational assessments. *Mol. Divers.* **2022**, *26*(1), 229–243.

62. Quan, N.V.; Xuan, T.D.; Tran, H.D.; Thuy, N.T.D.; Trang, L.T.; Huong, C.T.; Tuyen, P.T. Antioxidant, α-amylase and α-glucosidase inhibitory activities and potential constituents of *Canarium tramdenum* bark. *Molecules*. **2019**, *24*(3), 605.

63. Al-Rubaye, A.F.; Hameed, I.H.; Kadhim, M.J. A review: Uses of gas chromatography-mass spectrometry (GC-MS) technique for analysis of bioactive natural compounds of some plants. *Int. J. Toxicol. Pharmacol. Res.* **2017**, *9*(1), 81–85.

64. Prabhu, G.R.D.; Williams, E.R.; Wilm, M.; Urban, P.L. Mass spectrometry using electrospray ionization. *Nat. Rev. Methods Primers.* **2023**, *3*(1), 23.

Disclaimer/Publisher's Note: The statements, opinions and data contained in all publications are solely those of the individual author(s) and contributor(s) and not of MDPI and/or the editor(s). MDPI and/or the editor(s) disclaim responsibility for any injury to people or property resulting from any ideas, methods, instructions or products referred to in the content.